Moroccan Journal of Chemistry
ISSN: 2351-812X
http://revues.imist.ma/?journal=morjchem&page=login
Essifi & al. / Mor. J. Chem. 9 N°1 (2021) 142-155

Identification and quantification of the adsorption mechanisms of the cationic surfactant the cetylpyridinium chloride on Moroccan Na-montmorillonite

Kamal. Essifi[1]*, Mohammed.Nor[2], Doha. Berraaouan[1], El Houssien. Akichouh[2], Ali. El Bachiri[1], Allal. Challioui[2], Abdesselam. Tahani[1]*

[1]Laboratory of Physical Chemistry of the Natural Resources and Environment, Department of Chemistry, Faculty of Sciences, University Mohamed Premier, Oujda, Morocco
[2]Laboratory of macromolecular organic chemistry and natural products, Department of Chemistry, Faculty of Sciences, University Mohamed Premier, Oujda, Morocco

** Corresponding author:*
kamal.essifi.lpapc@gmail.com
Received 30 Oct 2020,
Revised 07 Feb 2021,
Accepted 10 Feb 2021.

Abstract

The modification of the clays (montmorillonite) by surfactants finds several applications in various fields, such as cosmetics, drugs, nanomaterials, etc. The experimental and the simulation of the adsorption of the cetylpyridinium surfactant on a Moroccan Na-Montmorillonite-type clay surface have been investigated. The adsorption rate of cetylpyridinium reached 2 CEC (Cation Exchange Capacity) and the maximum amount of adsorption increases for co-ion Br^- more than Cl^-. These results have been proven and we can conclude that the amount of adsorption varies according to the surfactant critical micelle concentration (CMC). The simulation shows the arrangement of the cationic surfactant's ions adsorbed on the basal surface. Where the cetylpyridinium are organized in two layers in a bimolecular and paraffinic manner. The binding coefficients for the formation of neutral complexes of either cationic surfactant's ions and the clay are calculated by a theoretical model and the binding force of the cationic surfactant ion on the surface of the clay depends on the co-ion. The FT-IR and XRD analyses showed that the surfactant is in strong interaction with montmorillonite for a surfactant adsorption rate lower than the CEC, and that the orientation of the surfactant molecules on the surface of the clay changes with the amount adsorbed to CP-Cl, especially for an adsorbed amount greater than the CEC.

Keywords: Adsorption isotherms, Montmorillonite, Binding coefficients, Simulation, Cationic surfactant.

1. Introduction

Clays are widely used in many scientific applications due to their natural availability and their ability of chemical and physical modifications. High cation exchange capacity and swelling capacity are characteristics that make clays very desirable in many industrial and scientific applications [1–4]. The inorganic ions in the clay can be replaced by salts of organic amines to form organo-clays [5–7]. Montmorillonite consists of 2: 1 layers [8], between which there are exchangeable hydrated ions. Each layer is composed of an octahedral sheet surrounded by two tetrahedral leaves (T. O.T) [9]. The octahedral sites are mainly occupied by Al^{3+}, but one part substituted by Fe^{3+} and Mg^{2+}. The tetrahedral montmorillonite sites normally contain Si^{4+} as central atoms with an Al^{3+} substitution, resulting in negative charge of surface sheets. The adsorption of cationic surfactants on the clay at the solid-liquid interface is a great technological interest and fundamental importance studied by several experimental techniques [5,10–12]. The adsorption of surfactants on the clay surfaces in aqueous medium is mainly governed by electrostatic and hydrophobic interactions [12–14], which include both the interaction between the surfactant and the surface and the mutual interaction between the surfactant molecules. The main factors involved are (a) electrostatic interactions between surfactant charged polar heads and surface (b) interaction between tails and (c) electrostatic repulsion between charged polar heads. At low coverage, surfactant cations physically adsorb in the form of individual ions at negatively charged surface sites. In this first stage of the adsorption process, the surfactant cations exchange with exchangeable cations of the clay or protons present at the solid-liquid interface [6,15]. This exchange depends on the properties of the solid-liquid interface and the type of surfactant [6,16]. Once the surface charge has been compensated, the electrostatic force for the adsorption of the surfactants will be canceled and the adsorption will only increase if the low affinity of the hydrophobic part of the surfactant for water can favor the auto-association and consequently the adsorption [12,17]. Researchers have discussed different investigations on the adsorption of variety of organic surfactants on montmorillonite such as cetyltrimethylammonium (CTA^+), cetylpyridinium (CP^+) to find out the adsorption phenomena [16,18,19], the arrangements of surfactants with each other and also with the surface of montmorillonite. Inadequate experimental evidences due to low montmorillonite crystallinity describes the computational simulation. Many works have shown that the negative charge of montmorillonite is compensated by organic surfactants, and those can be exchanged to obtain a modified montmorillonite with a different interlayer spacing. Meleshyn et al. [20] showed that the anions (Cl^-, I^-, Br^-) that usually compensate the cationic surfactant (CP^+) charge prefer the formation of pairs with inorganic cations rather than organic ones. Although, Pospíšil et al. [21] have simulated a dehydrated CP^+/montmorillonite system by applying a dynamic approach as a combination of the energy minimization and the NVE molecular dynamic methods where methyl-, methylene-, and head groups of the organic surfactants were represented as single interaction points. Despite the vast advance carried out the montmorillonite adsorption mechanism research, it is still a challenge to fully understand the factors that influence the selective adsorption of CP^+ on the surface of montmorillonite. Recently, molecular simulation has been proved to be a powerful technique to probe the detailed information about molecular arrangements and layering structure [22–24]. The simulated results provide not only the complementary evidence for the experimental results but also new insights for the microstructure of organoclay. For example, molecular simulation has demonstrated a mixed structure of paraffin-type and trilayer or quadrilayer in organoclay [24], which has never been discussed in experimental studies. This reflects that the real structure of organoclay is more complicated than those proposed on the basis of the experimental measurements. In this study, molecular simulation was used to determine the arrangement of surfactant molecules in the basal spacing obtained experimentally on the basis of minimum energy. A comparison was made between the simulated and experimental results, mainly in terms of the interaction of the surfactant cation (CP^+). To the author's knowledge little or no work has been reported that quantifies the mechanism of adsorption of the cationic surfactant by Moroccan montmorillonite.

The aim of the present study was to assess, quantitatively and qualitatively, different mechanisms of interaction between a cetylpyridinium type cationic surfactant and the surface of a Moroccan Na-Montmorillonite-type clay mineral, and to study the effect of ion and alkyl chain on the adsorption process. The experimental and the simulation of the adsorption of the cationic surfactant (cetylpyridinium chloride, CP-Cl) on a hydrophilic smectite (montmorillonite) surface has been investigated. The effect of the alkyl chain was studied, the pyridinium hydrochloride (PH-Cl) was taken as the polar head. The influence of the co-ion was also be studied by taking as adsorbates, the surfactant cetylpyridinium bromide (CP-Br) and its polar head hydrobromide pyridinium (PH-Br). The coefficients binding of the first stage of adsorption of the positively charged (CP-Cl) by the cationic exchange on the negatively charged montmorillonite was determined.

2. Materials and methods

The materials used for adsorption study are sodium montmorillonite, 1-cetylpyridinum chloride (CP-Cl) with the purity of > 98% (from HIMEDIA, RM1526-100G), 1-cetylpyridinum bromide (CP-Br) with the purity of > 98% (from SIGMA-ALDRICH, 202869-92-9), pyridinium hydrochloride (PH-Cl) and pyridinium hydrobromide (PH-Br) (from ACROS ORGANICS, 628-13-7). In Figure1, the chemical structure of surfactant cetylpyridinium and its polar head hydro-pyridinium. Na-montmorillonite from Nador (Morocco) was used, it was purified and sodium exchanged before used. The unit cell formula was $[Si_{7.97}Al^{3+}_{0.03}]^{IV}[Al^{3+}_{2.737}Fe_{0.221}Mg_{1.157}]^{VI}O_{20}(OH)_4(Na_{0.722}Ca_{0.056})$ (The Roman numerals IV and VI on the cells designate the octahedral and tetrahedral sites respectively) [25,26]. The Suspensions of 10 g/l sodium montmorillonite are prepared by dispersing 5 g of montmorillonite-Na in 500 ml of distilled water. The suspensions was stirred for more than 48 hours to better disperse and for homogeneous mixture of montmorillonite.

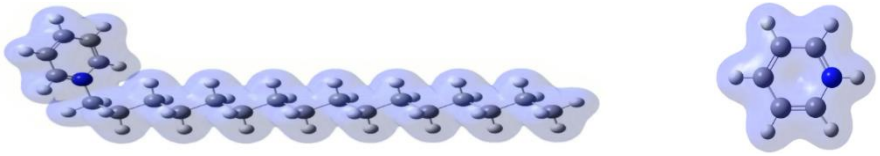

a **b**

Figure1. (a) Optimized geometry of CP-Cl molecule, (b) Optimized geometry of the PH-Cl molecule, visualized with Gauss View. The quaternary nitrogen atom is shown in blue, the gray spheres indicate carbon atoms, and the white spheres indicate hydrogen atoms.

2.1. The determination of the Critical Micellar Concentration of CP-Cl surfactants

The critical micelle concentration (CMC) and the cross-sectional area of the polar head group at the water/air interface (Am) at 25 °C were determined by applying the Gibbs equation to the surface tension measurement with an electrobalance type tensiometer (GIBERTINI TSD). This instrument follows to have the static measure of the surface tension of liquid samples with the Wilhelmy plate method after a calibration with distilled water. Briefly, a series of a sample with different concentrations of surfactant are prepared and placed in the container of TSD instrument and lifted until the surface is close to the lower side of the plate, we press the ZERO key to make the tensiometer ready to execute the measure, after the very slow lift, when the sample's surface touches the lower side of the plate, a meniscus is formed. The value showed on the display is the surface tension of the sample.

The appropriate form of Gibbs adsorption equation for the ionic surfactants used to determine the surface excess concentration of surfactant ions Γ_s is the following equation:

$$\Gamma_s = \frac{1}{2RT}\left(\frac{d\gamma}{d\ln C}\right)$$

Where γ is the surface tension (mN/m) and **C** is the concentration of surfactant in the bulk phase (mol/l).

2.2. Measurement of cation exchange capacity (CEC) of Na-montmorillonite

The cation exchange capacity (CEC) of the clay defined as the total amount of exchangeable cations that the clay can adsorb was estimated by a method based on the adsorption of $CuCl_2$ $(EDA)_2$ copper complexes [27]. The principle of this method is as follows: 300 mg of the clay dehydrated at 120 °C, 10 ml of complex and 10 ml of distilled water were mixed in one tube. The mixture stirred for 24 hours and then centrifuged for 10 min at 7000 rpm. Then, the supernatant was analyzed by UV-vis for the purpose of measuring the concentration of the remaining complex at equilibrium, the $[Cu\ (EDA)_2]^{2+}$ complex absorbs at λ_{max} = 548 nm strongly. The CEC of the purified sodium montmorillonite was 90 meq/100 g.

2.3. Fourier Transform Infrared Analysis (FT-IR)

Fourier Transforms Infrared (FT-IR) spectra were obtained by IR Prestige 21, Shimadzu using KBr disks and the samples were scanned in a wave number range of 4000cm^{-1} to 400 cm^{-1} with an average of 30 scans and a resolution of 4 cm^{-1}. All FT-IR spectra were recorded and analyzed for the nature of the binding of the functional group.

2.4. X-ray Measurements

The compositions of the specimens were determined using X-ray diffraction (Shimadzu XRD-6000) using monochromatic CuKα at a voltage of 40 KV and an intensity of 40 mA. The diffraction angle was continuously scanned in the 2θ range of 3–15 ° at a scanning rate of 2 deg/min. The measured distances d (00l) are determined with Match 3.3 software. For this analysis, organoclay was dried at 50 °C, crushed using an agate mortar, and directly put into the sample holder.

2.5. Adsorption Isotherm

The adsorption isotherms were determined using the residue method [15]. Briefly, 5 ml of the homogeneous suspension of colloidal clay (10 g/l) was placed in a PTFE flask. To this was added 20 ml of calibrated solution of surfactants. The pH of the initial solutions was in the range [5.5-6.3]. Then the mixture was stirred conveniently for 24 hours at 25 °C to achieve equilibrium. To determine the adsorption isotherm, the samples were centrifuged in an ultracentrifuge for 15 minutes at 10,000 rpm to separate the clay particles. The remaining surfactant concentration in the supernatant was determined by UV-Vis spectrophotometry (MACY UV-1100) at 260 nm.

The adsorbed amount was calculated using the equation:

$$Q_{ads} = (C_0 - C_{eq}).\frac{V}{m}$$

with: $\mathbf{C_0}$ the initial surfactant concentration (mol/l), $\mathbf{C_{eq}}$ the equilibrium surfactant concentration, **V** (l) the total volume of the sample, **m** (g) the mass of clay used and $\mathbf{Q_e}$ the amount of surfactant adsorbed per gram of clay (mol/g).

2.6. Simulation details

The annealing simulation in the canonical ensemble (constant atom number, volume and energy [NVE]) was utilized to understand the mechanism of adsorption of CP-Cl, and to determine the arrangement of surfactant molecules in the basal spacing obtained experimentally on the basis of minimum adsorption energy of CP-Cl on the surface of montmorillonite (001). The vacuum slab with 4a×3b×1c crystal unit was created and the vacuum slab was orientated along the c-plane with vacuum thickness of 20 Å, crystal thickness of 27.7 Å and position of 1 Å to position the crystal within the portion of vacuum slab, the CP-Cl was limited to 13 monomers in respecting the total interlayer charge compensates the total mineral layer charge (-13e) in the simulation box (13 correspond to the interlayer CP+ content to 100% CEC). Adsorption locator was used to generate the models depicting CP-Cl on the surface of

montmorillonite crystal. All adsorption locator calculations were performed using compass force field with the surface region defined by atom set, and with the fixed number of 10 configurations. The interaction energies between CP-Cl and montmorillonite crystal surface was calculated. All simulations were executed using the adsorption locator and forcite Modules of Materials Studio (version 17.1.0.48). The force field used is COMPASS 2, the system was subjected to energy minimization for geometry optimization before anneal simulations were conducted. For minimization calculation a maximum iteration of 50,000 was used with an ultra-fine convergence level. The anneal simulation using NVE lasted for $5 \cdot 10^{-12}$ seconds (ps) with a time step of 10^{-15} seconds (fs). All results were collected at last.

3. Results and discussions

3.1.The determination of the Critical Micellar Concentration of CP-Cl and CP-Br

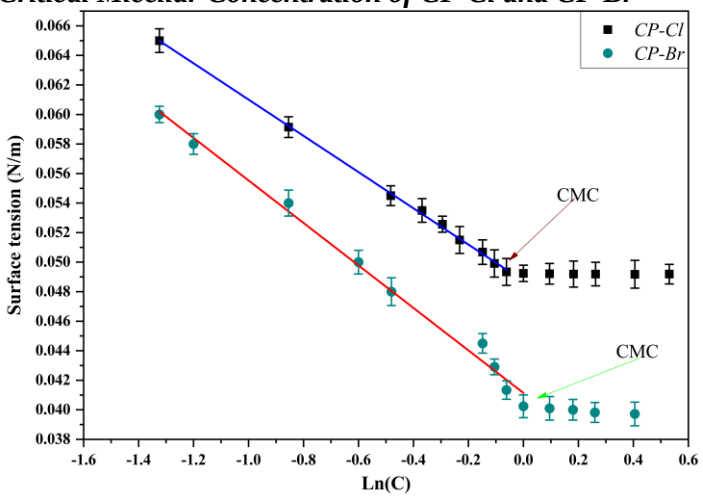

Figure 2. The variation of the surface tension of aqueous solutions of CP-Cl and CP-Br against the logarithm of surfactant concentration.

In figure 2, the surface tension of the surfactant solutions CP-Cl and CP-Br, respectively, as a function of their concentration decreases and remains almost constant for a CMC equal to 0.955 mmol/l and 1 mmol/l respectively. The variation of the surface tension as a function of the concentration of the surface-active agent before the CMC will be used to determine the excess charge on the surface, which makes it possible to estimate the surface occupied by a surfactant molecule. The area occupied by a surfactant molecule is given by:

$$A_m = \frac{10^{20}}{N_A \Gamma_0} \quad (Å^2/molecule)$$

The surface area values per molecule obtained are shown in Table 1. For CP-Cl and CP-Br cationic surfactants with the same head group area, but with a different counter ion, the surface area values per molecule different from one chloride counter ion to one bromide counter ion, these results show good agreement with the reported value Mata et al [28].

Table 1. Critical Micellar Concentration and the Area per Molecule for Surfactant at the Air-Liquid Interface.

Surfactants	CMC (mmol/l)	Area per molecule ($Å^2$)	References
CP-Cl	0.955	67	This work
CP-Br	1	58.57	This work
CTAC	1.25	54	[28]
CTAB	0.98	51.7	[28]

3.2.Adsorption Isotherm

Figure 3 presents the adsorption isotherm of the surfactant CP-Cl, the appearance of the isotherm is characterized by two regions: the first of high adsorption for very low values of surfactant concentrations up to an environmental adsorption value of 0.8×10^{-3} mol/g resulting from a cation exchange between the surfactants and the exchangeable cations (sodium cations) of the clay; the second region begins after the CEC of the clay, the amount of adsorbed surfactant molecules increases gradually, the latter characterizes the hydrophobic adsorption by the alkyl chains [29,30]. Then a plateau is obtained after CMC (0.955 mmol/l), for which the chemical potential of the monomers remains constant.

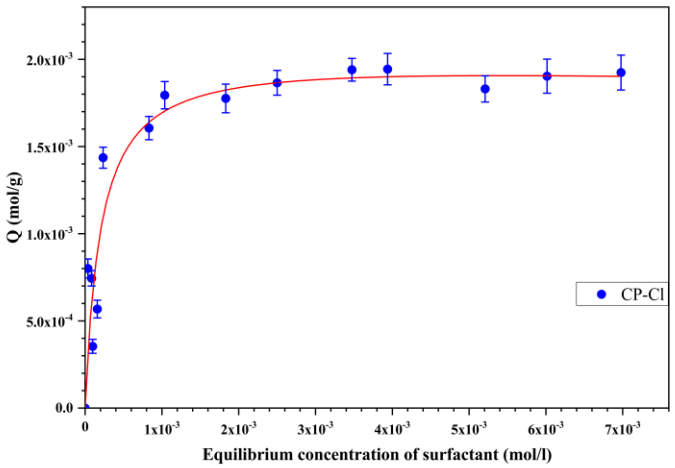

Figure 3. Adsorption isotherm of cationic surfactant CP-Cl on Na-montmorillonite for $\frac{S}{L} = 0.2\%\ (w/w)$.

3.3.Influence of the Alkyl Chain

Figure 4 presents the comparison of the adsorption isotherms of the cationic surfactant CP-Cl and its polar head PH-Cl as a function of their concentration at equilibrium. The maximum adsorption amount of CP-Cl is practically 2.13 times greater than that of PH-Cl. This explains the important role of the alkyl chain (hydrophobic part) of the cationic surfactant in the adsorption [29–31]. Indeed, the influence of the apolar part on the adsorption process is taken into consideration only from a chain length exceeding 8 carbon atoms [32]. Several authors have shown that as the length of the chain increases, the maximum adsorbed quantity increases, this correlation explained by the fact that the longer the chain length increases the greater the hydrophobic effect, which favors the solution micellization and consequently the adsorption [30,32,33].

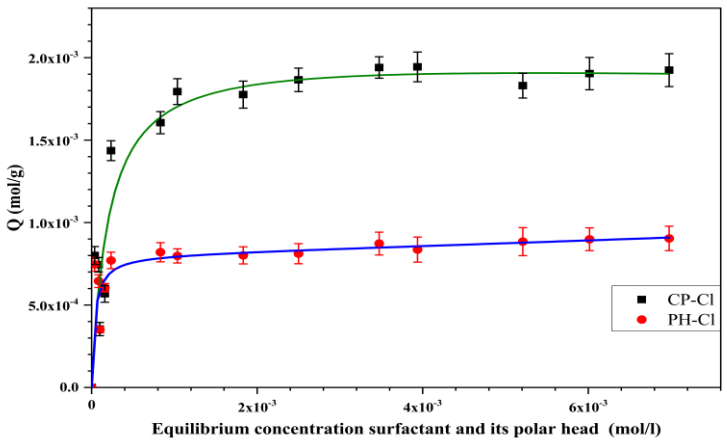

Figure 4. Adsorption isotherm of CP-Cl and its polar head PH-Cl on Na-montmorillonite for $\frac{S}{L} = 0.2\%\ (w/w)$.

3.4.Influence of co-ion

Figures 5 and 6 respectively presents the adsorption isotherms of pyridinium hydrobromide (PH-Br), pyridinium hydrochloride (PH-Cl), the adsorption isotherms of cetylpyridinium bromide (CP-Br) and Cetylpyridinium chloride (CP-Cl). The results show that the effect of the co-ion on the adsorption for the surfactants or the polar heads is translated by an increase of the quantity of molecules adsorbed to the surface when passing from the chloride ion (Cl^-) to the bromide ion (Br^-). Boyd et al [34], explained this effect of the co-ion by increasing the polarizability of the ion and consequently the increase of the screening effect which increases the charge of the polar head of the surfactant, hence the increase in the maximum adsorbed amount of CP-Br relative to the CP-Cl and PH-Br relative to PH-Cl.

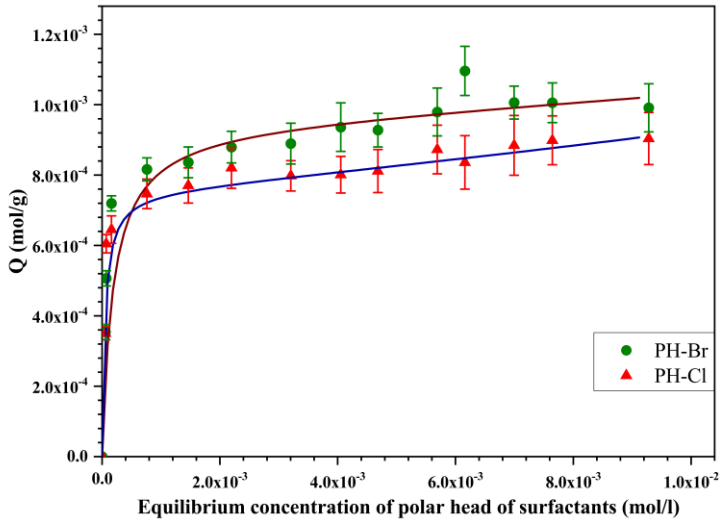

Figure 5. Adsorption isotherm of PH-Br and PH-Cl on Na-montmorillonite for $\frac{S}{L} = 0.2\%\ (w/w)$.

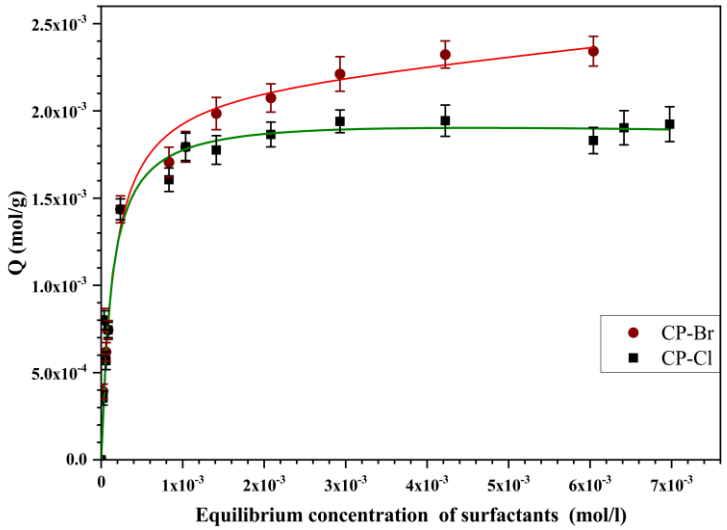

Figure 6. Adsorption isotherm of PH-Br and PH-Cl on Na-montmorillonite for $\frac{S}{L} = 0.2\%\ (w/w)$.

3.5.Model calculations

The binding coefficients were determined for concentrations below the CMC as described by Nir [35], Margulies et al. [36], Nir et al. [37], Akichouh et al. [15]. The programs consider cation binding, the electrostatic Gouy-Chapman equations, and solve iteratively for the solution concentrations of all cations in a closed system. The equations of the exchange and of the binding coefficient are given below.

$$BE - Na^+ + (CP^+, Cl^-) \leftrightarrow\ BE - CP^+ + (Na^+, Cl^-)$$

With a binding coefficient K, given by:

$$K = \frac{[BE - CP^+]}{[BE^-][CP(0)^+]}$$

In which $[CP(0)^+]$ is the concentration of the cation surfactant at the surface and $[BE^-]$ is the singly charged negative site, on the surface of the montmorillonite. The binding coefficients of the inorganic cations in the system were taken from the previous studies (Nir et al., 1986; Rytwo et al., 1996) [38,39]. For CP^+ cationic surfactants the intrinsic binding coefficient K for the formation of neutral complexes was determined from adsorption data. Table 2 presents the results obtained.

Table 2. Binding Coefficients of cationic surfactants CP-Cl and CP-Br and sodium cation Na^+.

Surfactants	K (M^{-1})	Reference
CP-Cl	11500	This work
CP-Br	12000	This work
Na^+	1	[40]

The K binding coefficient for CP^+ is high for both types of co-ions that illustrate its high affinity for the clay. So, this binding coefficient is higher for CP^+ Br^- compared to that of CP^+ Cl^- indicating the co-ion binding effect of the surfactant to the clay surface. The more electronegative and polarizable the co-ion is, the greater the surface binding coefficient, which in turn implies higher adsorption.

3.6. Results/Properties of adsorbent-adsorbate complex (Montmorillonite-CP-Cl)

Figure 7 presents the FT-IR Spectra of Na-montmorillonite and CP-Cl-modified montmorillonite at different clay surface coverage rates. The IR spectra of the different complexes confirm the presence of surfactant molecules on the surface of sodium montmorillonite by the appearance of the absorption bands corresponding to NH elongations, vibrations asymmetric elongations of CH_2 and CH_3 of the alkyl chain and absorption bands corresponding to the aromatic ring C=C elongations of the polar head in addition to the absorption bands of pure Na-montmorillonite. It is also noted a widening of the peak at 1031.95 cm^{-1} corresponding to the Si-O group due to the overlap of the valence vibration absorption bands of the Si-O bond and the C-N elongation of the CP-Cl surfactant.

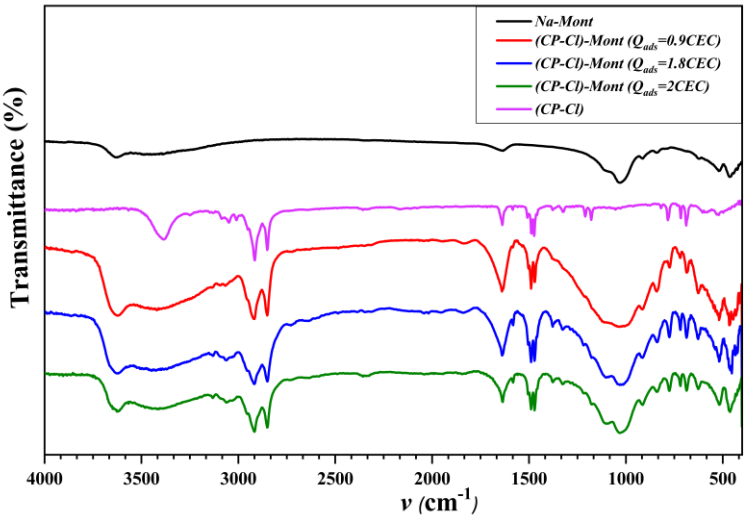

Figure 7. FT-IR Spectra of Na-Montmorillonite and the Bent- CP-Cl Complex for Different Coverages.

The FT-IR spectra of the various complexes and of the powdered CP-Cl surfactant shows a displacement of the CH_2 vibration absorption band of the alkyl chain as a function of the adsorbed amount of CP-Cl. The vibration band of CH_2 moves from 2914.54 cm^{-1} for the powdered CP-Cl surfactant to 2918.40 cm^{-1} for the complex where the adsorption rate is lower than the CEC. This displacement shows that the orientation of the alkyl chain is perturbed by its

adsorption on the clay surface, which confirms that the adsorption of the surfactants in the interspace of the clay mineral is produced by a "strong" adsorption mechanism, in which the surfactant is adsorbed by an exchange of the interlayer inorganic cation (Na^+) with an organic cation (CP^+). For quantities of adsorption greater than the CEC of the clay, the displacement is reversed, that is to say the vibration band of CH_2 moves to low values of the wave number [16,41], justifying the reorientation of the alkyl chain with respect to the surface which is favored by an interaction between the alkyl chains. This confirms the existence of a "weak" adsorption mechanism of the Van der Waals-type interactions between the carbon residues of the surfactant molecules in solution and the molecules previously adsorbed by the "strong" mechanism. Hexadecyltrimethylammonium (HDTMA) bromide adsorption studies on Wyoming montmorillonite (SWy) and Arizona montmorillonite (SAz), show that the interlayer structure of montmorillonite varies with the amount of HDTMA adsorbed in different ways for different montmorillonite [18,33].

3.7.Analysis of Adsorption Layer by X-ray diffraction

For a maximum adsorption rate, the X-ray results (figure 8) shows that the basal distance d_{001} of the sodium montmorillonite increases by a distance equal to 8 Å ($d_{001} = 20.6$ Å) and 7.72 Å ($d_{001} = 20.32$ Å) in the case of modification with cetylpyridinium chloride and cetylpyridinium bromide surfactants respectively, these results are in agreement with the literature [20]. The adsorption of the surfactant molecules or cations on the clay has different structures depending on the cation exchange capacity of the clay (CEC), the length of the alkyl chain or the method of preparation. These molecules or cations can adopt various dispositions in the interlamellar spacing of clay [33,42,43]. The orientation and clustering density of surfactant molecules between clay sheets can be deduced from X-ray data combined with quantitative measurements of adsorption [17]. The thickness of the anhydrous montmorillonite sheet is 9.5 Å, the estimated geometric volume for the CP-Cl surfactant is approximately 621 $Å^3$. The apparent packing area of the CP-Cl, as calculated from the plateau region of the adsorption isotherm, is about 65 $Å^2$, so the estimated thickness of the CP-Cl surfactant is 9.5 Å, which is equal to the interlamellar distance obtained by X-ray measurements, (9.5Å). In this case, the cationic surfactants in the interlamellar space would form an alternating monolayer, whose surfactant molecules are slightly inclined with respect to the basal plane [41]. The molecules of surfactants inserted into the interlamellar space for an adsorption rate lower or equal to the CEC of the montmorillonite according to a cation exchange mechanism, would form a flat monolayer [20]. After the CEC and according to some researchers [12,34], the cationic surfactants begin to organize into bilayers whose alkyl chains are linked by hydrophobic attractions, and according to the previous calculations, these surfactant cations would form a bilayer flat [20]. Tahani et al. [17], show that the adsorption of the co-ions (Cl^- or Br^- ions) starts just after the CEC; that is to say after the CEC of the clay, there is a simultaneous adsorption of cationic surfactant-co-ion pairs. Indeed, the adsorption of the counter-ion decreases the repulsion between the charged surfactant heads, and leads to a higher adsorption until the saturation of the interlamellar space is reached. And therefore, there is a rearrangement of the surfactant molecules, which confirms the results of IR analyses. In this case, the surfactant molecules adopt a slightly paraffinic structure inclined with respect to the basal plane, which will subsequently show by the simulation of the adsorption of the cationic surfactant (CP^+). Increasing the hydrophobicity of the surfactant from a Cl^- to Br^- co-ion result in an increase in the adsorption rate, and therefore the CP-Br surfactant molecules would form a dense and more compact bilayer than that formed by the CP-Cl molecules. So, the reorganization of the surfactant structure layer adsorbed on the clay can change the reorganization of the clay particle [18,44]. The adsorption of the polar heads of pyridinium chloride and pyridinium bromide lead to an increase in the basal distance of 4.3 and 4.53 Å respectively. If we take as approximations the Van der Waals distance of the 4 Å methylene group, the possible structure adopted by the pyridinium cations in the adsorption layer is a monolayer whose cations are slightly tilted relative to the basal surface of the clay.

Based on the Lagaly model [45], the different possible configurations adopted by the different molecules adsorbed in the interlamellar space are presented in the Table 3.

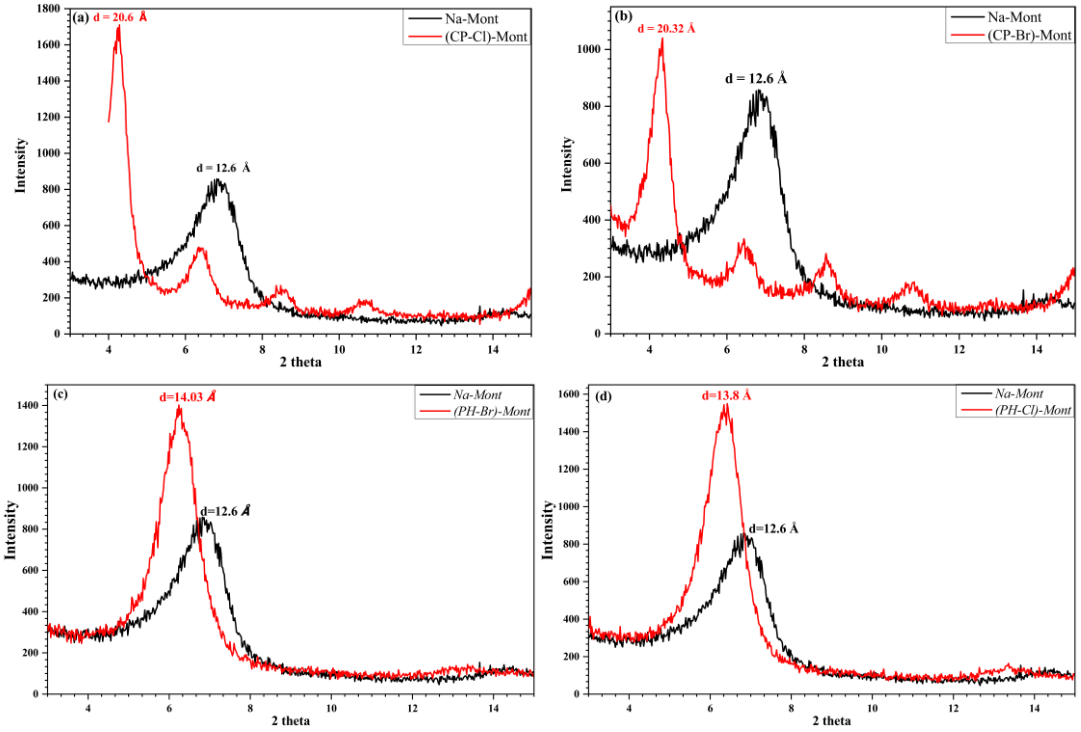

Figure 8. X-ray spectra of organoclays Montmorillonite-CP-Cl (a), Montmorillonite-CP-Br (b), Montmorillonite-PH-Br (c) and Montmorillonite-PH-Cl (d).

Table 3. Structure of the adsorption layer for different molecules adsorbed for a maximum rate on montmorillonite.

Adsorbed molecule	**Adsorption rate**	d_{001}(Å)	Δd^* (Å)	**Orientation of the adsorbate relative to the basal surface of the clay**	**Arrangement of adsorbed molecules**
CP-Cl	1.7 CEC	20.6	11.1	tilted	Alternate bilayer
CP-Br	2 CEC	20.32	10.82	tilted	Alternate bilayer
PH-Cl	0.8 CEC	13.8	4.3	slightly tilted	------
PH-Br	1 CEC	14.03	4.53	slightly tilted	-------

3.8.Interlayer Arrangement and Conformation of CP^+ cations

The energy terms calculated by the anneal optimization of CP^+ on montmorillonite (001) surface are regrouped in table 1, the interaction energy of CP^+ to montmorillonite (001) surface is calculated by the equation:

$$E_{interaction} = E_{total} - (E_{surface} - E_{CP^+})$$

The value of the negative interaction energy indicates the attractive interactions between the CP^+ and the surface of the montmorillonite. These interaction energy values show that the CP^+ surfactants interact strongly and favorably on the surface of the montmorillonite (001) with an upper interaction energy equal to -1794.485905 kcal/mol. The negative value of the potential energy (-572.050979 kcal/mol) indicates that the adsorption process is highly favorable in terms of energy. High negative non-bond energy, Van der Waals energy, and electrostatic energy also indicate the role of the interaction of cationic surfactant (CP^+) with the surface of montmorillonite on the growth of the CP^+ layer in the basal clay surface.

Table 4. The output energy terms calculated by the anneal optimization of CP-Cl on montmorillonite (001) surface.

Interaction energy (kcal/mol)	Total potential energy (kcal/mol)	Bond energy (kcal/mol)	Angle energy (kcal/mol)	Torsion energy (kcal/mol)	Inversion energy (kcal/mol)	Van der Waals energy (kcal/mol)	Electrostatic energy (kcal/mol)	Total valence energy (kcal/mol)	Non-bond energy (kcal/mol)
- 1794.485905	- 572.050979	305.9687678	532.4419259	- 520.5328824	- 8.37825893	- 168.4844849	-689.222419	326.2560702	- 865.5148798

Figure 11 presents the arrangement of the surfactant molecules (CP^+) in the interlayer space with a CP^+ content of 100% CEC in the equilibrium state. Detailed characterization of the interlayer structure can be achieved using interlayer density profiles and pair distribution functions. The figure 9, represented the concentration profiles of N-CP^+, C-CP^+ and Mg-montmorillonite in a given layer or stripe, the values range from 0 (no particles in the layer or stripe) to a maximum value corresponding to the total number of bins, if all atoms of each N-CP^+, C-CP^+ and Mg-montmorillonite reside in the same layer or stripe, the two vertical lines at the distances 1.86 and 7.79 Angstrom (Å) represents the area occupied by the montmorillonite layer. The results obtained show a correlation between the positions N and Mg between the axis (010) and symmetrically between the axis (100), which indicates that the adsorption mechanism of the CP^+ translated by attractive interactions between the associated positive charges to the nitrogen atoms and the negative charges associated with the sites containing the Mg atoms. A similar result was reported [19,22,46]. The minimum distance between Mg and N is 5.35 Å based on the radial distribution function of N-CP^+ around Mg in CP^+ modified montmorillonite (Figure 10). The distance between the CP^+ pyridinium heads and the montmorillonite surface (001) along the z axis was 0.8 A, the pyridinium cycle of the cationic surfactant pointing towards the surface as shown in concentration profiles of the C-CP^+ and the N-CP^+, the ratio C-CP^+ by N-CP^+ approximately equal to 5 at z equal 10.1 and 27.2 Å, this is due to the delocalization of the positive charge on the pyridinium cycle.

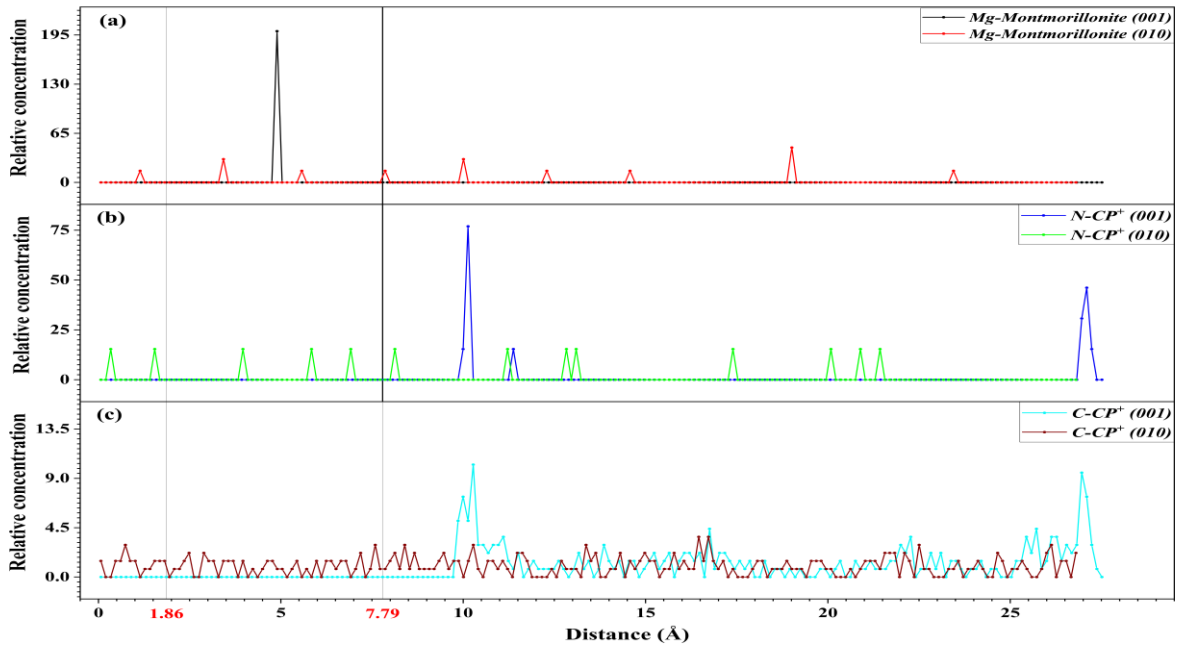

Figure 9. The concentration profiles of Mg-montmorillonite (a), N-CP^+ (b) and C-CP^+ (c) as functions of themselves position (Å) along y (010) and z (001) axis.

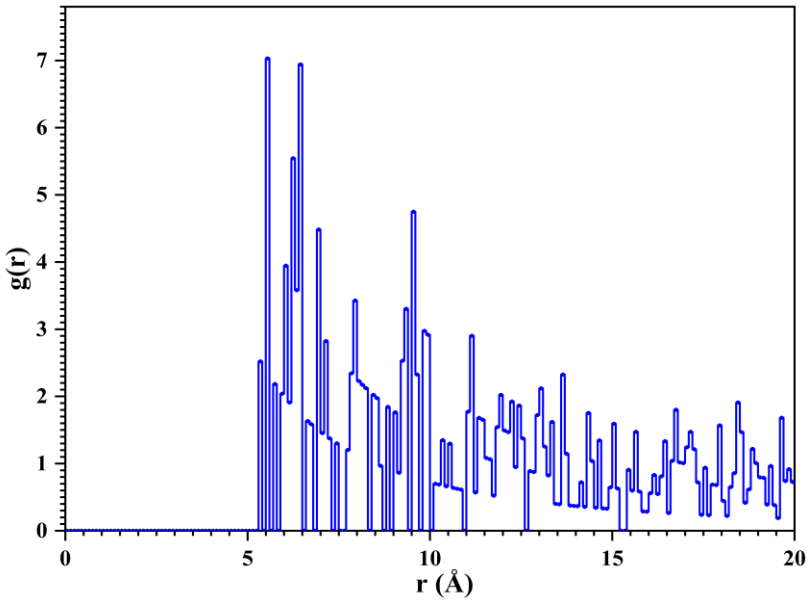

Figure 10. Radial distribution function g(r) for N-CP^+ around Mg in CP^+-modified montmorillonite.

The characteristic interlayer structures (figure 11) show the aliphatic chains of CPC surfactants fill the entire interlayer spacing with the existence of parallel-chains arrangements at 100% CEC and the pyridinium rings occupied the area near the montmorillonite surface, composing a bimolecular-like form. Overall, CP^+ surfactants organized in two layers in a way between bimolecular-like and paraffin-like which go well with the experimental results founded. This obtained results are consistent with the experimental observations by the use of advanced techniques (FTIR and XRD). The results obtained are consistent with the suggestion deduced from the FTIR, NMR and XRD spectra [20,43,47–49]. The unit cell formula obtained of the montmorillonite modified by the cationic surfactant CP^+ was $[Si_{7.97}Al^{3+}_{0.03}]^{IV}[Al^{3+}_{2.699}Fe_{0.217}Mg_{1.157}]^{VI}O_{20}(OH)_4(CP^+_{1.083})$.

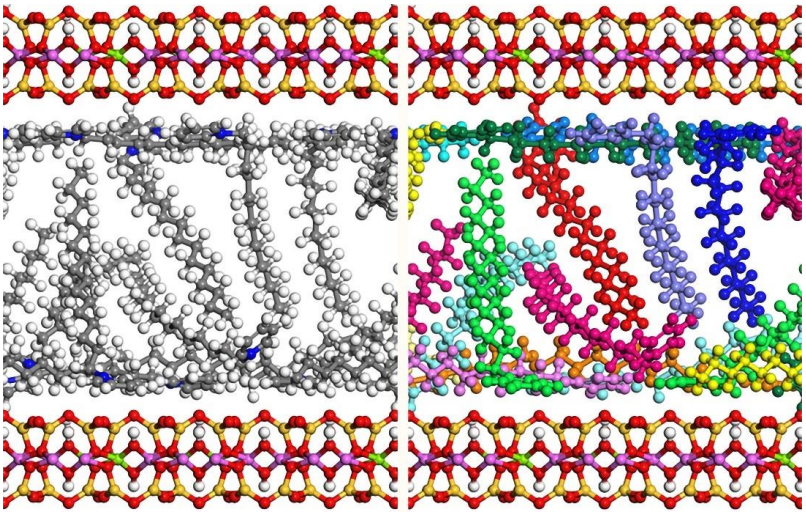

Figure 11. (a) modified montmorillonite (~20 Å), arrangements of interlayer CP^+ ions in dehydrated montmorillonite (side view). Ball and stick colors: blue (N), grey (C), red (O), white (H), green (Mg), purple (Al), gold (Si). (b) each CP^+ surfactants own different colors to distinguish their conformations.

4. Conclusion

The adsorption of the surfactant (CP-Cl) in aqueous solution on clay suspensions (Na-montmorillonite), showed that the rate of adsorption of flat to tilted monolayer of the surfactant cations on the surface does not go over the CEC of

the clay (low surfactant concentrations), there is a strong adsorption which is translated by a cation exchange between the adsorbate and the exchangeable sodium ions of the clay. The binding coefficient (K) corresponding to the CP-Br is higher compared to those of CP-Cl indicating the co-ion binding effect of the surfactant to the clay surface. After the exchange and from an adsorption rate equal to the CEC of the sodium montmorillonite, the adsorption corresponds to adsorption by the lateral interactions between the alkyl chains. This is confirmed by the study of the adsorption of the polar head PH-Cl, for which adsorption stops at the CEC. The adsorption reaches 2 CEC for CP-Br and is lower for the CP-Cl (1.7 CEC). Along the factors studied which influence the adsorption of the surfactants, the results obtained show that the maximum amount of adsorption increases from Cl to Br. The use of IR spectroscopy and Diffraction X-ray for the determination of the structure layer of adsorbed (CP-Cl) on Na-montmorillonite shows that the surfactant is in strong interaction with montmorillonite for a surfactant adsorption rate lower than the CEC, and that the orientation of the surfactant molecules on the surface of the clay changes with the amount adsorbed to CP-Cl, especially for an adsorbed amount greater than the CEC. The cationic surfactant adsorption simulation results, cetylpyridinium, confirm the arrangement of the surfactant molecules in the interlamellar space of the montmorillonite obtained by the combination of the quantitative adsorption calculation results, FTIR and the XRD data.

Acknowledgments

The authors are sincerely thankful to MESRSFC and CNRST—Morocco for their financial support of Project PPR 15–17. The authors are thankful to Professor Abdelmonaem Talhaoui, Head of Department of Chemistry, University of Mohammed first Oujda, for his help with the physical and chemical analysis.

References

[1] G. Dios-Cancela, L. Alfonso-Méndez, F.J. Huertas, E. Romero-Taboada, C.I. Sainz-Díaz, A. Hernández-Laguna, Journal of Colloid and Interface Science, (222) (2000) 125–136.

[2] A. Borrego-Sánchez, E. Gómez-Pantoja, E. Morillo, T. Undabeytia, C.I. Sainz-Díaz, Applied Clay Science, (161) (2018) 533–543.

[3] Y. Xi, R.L. Frost, H. He, T. Kloprogge, T. Bostrom, Langmuir, (21) (2005) 8675–8680.

[4] T.H. Mouna, M. Jendoubi, M. Ben Amor, M. Benna-Zayani, Moroccan Journal of Chemistry, (6) (2018) 135–147.

[5] Saranya Jagadeesan, Subramanian Chitra, Abdelkadar Zarrouk, Mor. J. Chem. 8 N°2(2020)446-473

[6] S. Nir, T. Undabeytia, D. Yaron-Marcovich, Y. El-Nahhal, T. Polubesova, C. Serban, G. Rytwo, G. Lagaly, B. Rubin, Environmental Science and Technology, (34) (2000) 1269–1274.

[7] W. H. Hoidy, M. B. Ahmad, E.A. Jaffar Al, N.A. Bt Ibrahim, Am. J. Appl. Sci., (6) (2009) 1567–1572.

[8] W.P. Hwu, J. M., Jiang, G. J., Gao, Z. M., Xie, W., & Pan, J. Appl. Polym. Sci., (83) (2002) 1702–1710.

[9] H. Jahan, S. A., Parveen, S., Ahmed, S., & Kabir, Materials Science, (8) (2012).

[10] G. Wang, S. Wang, Z. Sun, S. Zheng, Y. Xi, Applied Clay Science, (148) (2017) 1–10.

[11] *Hasna Bouhali, Nabila Chalal, Hadj HAMAIZI, Abdelkader Benguedach* DOI: https://doi.org/10.48317/IMIST.PRSM/morjchem-v3i4.3230

[12] J.M. Cases, F. Villieras, Langmuir, (8) (1992) 1251–1264.

[13] F.M. Flores, T. Undabeytia, E. Morillo, R.M. Torres Sánchez, Environmental Science and Pollution Research, (24) (2017) 14463–14476.

[14] F. Ding, M. Gao, T. Shen, H. Zeng, Y. Xiang, Chemical Engineering Journal, (349) (2018) 388–396.

[15] E.H. Akichouh, S. Salhi, M. Khoutoul, M. El Miz, A. El Bachiri, A. Tahani, Oriental Journal of Chemistry, (36) (2020) 63–75.

[16] N.M. Mahmoodi, A. Taghizadeh, M. Taghizadeh, M. Azimi, Journal of Environmental Chemical Engineering,

(7) (2019) 103243.
[17] A. Tahani, M. Karroua, H. Van Damme, P. Levitz, F. Bergaya, J. Colloid Interface Sci., (216) (1999) 242–249.
[18] S.Y. Lee, W.J. Cho, P.S. Hahn, M. Lee, Y.B. Lee, K.J. Kim, Appl. Clay Sci., (30) (2005) 174–180.
[19] P. Praus, M. Turicová, S. Študentová, M. Ritz, J. Colloid Interface Sci., (304) (2006) 29–36.
[20] A. Meleshyn, C. Bunnenberg, J. Chem. Phys. B, (110) (2006) 2271–2277.
[21] M. Pospíšil, P. Čapková, D. Měřínská, Z. Maláč, J. Šimoník, J. Colloid Interface Sci., (236) (2001) 127–131.
[22] Y. Yang, Z. Ma, F. Xia, X. Li, Journal of Water Process Engineering, (36) (2020) 101292.
[23] E. Hackett, E. Manias, E.P. Giannelis, J. Chem. Phys., (108) (1998) 7410–7415.
[24] Q.H. Zeng, A.B. Yu, G.Q. Lu, R.K. Standish, Chem. Mater., (15) (2003) 4732–4738.
[25] M. El Miz, H. Akichoh, D. Berraaouan, S. Salhi, A. Tahani, Am. J. Appl. Chem., (2017) (2017) 105–112.
[26] M. El Miz, E. Kamal, S. Samira, B. Faiza, Mor. J. Chem., (2) (2019) 242–253.
[27] F. Bergaya, M. Vayer, Appl. Clay Sci., (12) (1997) 275–280.
[28] J. Mata, D. Varade, P. Bahadur, Thermochimica Acta, (428) (2005) 147–155.
[29] Ö. Açışlı, S. Karaca, A. Gürses, Applied Clay Science, (142) (2017) 90–99.
[30] J.L. Trompette, J. Zajac, E. Keh, S. Partyka, Langmuir, (10) (1994) 812–818.
[31] M. Alkan, M. Karadaş, M. Doğan, Ö. Demirbaş, Journal of Colloid and Interface Science, (291) (2005) 309–318.
[32] Q. Yang, M. Gao, W. Zang, Colloids and Surfaces A: Physicochemical and Engineering Aspects, (520) (2017) 805–816.
[33] X. Hu, S. Tian, S. Zhan, J. Zhu, Applied Clay Science, (146) (2017) 140–146.
[34] S. Xu, S.A. Boyd, Langmuir, (11) (1995) 2508–2514.
[35] S. Nir, J. Colloid Interface Sci., (102) (1984) 313–321.
[36] L. Margulies, H. Rozen, S. Nir, Clays and Clay Minerals, (36) (1988) 270–276.
[37] S. Nir, G. Rytwo, U. Yermiyahu, L. Margulies, Colloid Polym. Sci., (272) (1994) 619–632.
[38] S. Nir, Soil Sci. Soc. Am. J, (50) (1986) 52.
[39] G. Rytwo, Clays and Clay Minerals, (44) (1996) 276–285.
[40] S. Nir, D. Hirsch, J. Navrot, A. Banin, Soil Sci. Soc. Am. J, (50) (1986) 40–45.
[41] S. Peker, S. Yapar, N. Beşün, Colloids and Surfaces A: Physicochemical and Engineering Aspects, (104) (1995) 249–257.
[42] K. Srinivasarao, S.M. Prabhu, W. Luo, K. Sasaki, Applied Clay Science, (163) (2018) 46–55.
[43] H. Othmani-Assmann, M. Benna-Zayani, S. Geiger, B. Fraisse, N. Kbir-Ariguib, M. Trabelsi-Ayadi, N.E. Ghermani, J.L. Grossiord, J. Chem. Phys. C, (111) (2007) 10869–10877.
[44] P.M. Naranjo, E.L. Sham, E.R. Castellón, R.M. Torres Sánchez, E.M. Farfán Torres, Clays and Clay Minerals, (61) (2013) 98–106.
[45] G. Lagaly, Solid State Ion., (22) (1986) 43–51.
[46] H. Heinz, H. Koerner, K.L. Anderson, R.A. Vaia, B.L. Farmer, Chemistry of Materials, (17) (2005) 5658–5669.
[47] L.Q. Wang, J. Liu, G.J. Exarhos, K.Y. Flanigan, R. Bordia, J. Chem. Phys. B, (104) (2000) 2810–2816.
[48] H. He, Z. Ding, J. Zhu, P. Yuan, Y. Xi, D. Yang, R.L. Frost, Clays and Clay Minerals, (53) (2005) 287–293.
[49] H. He, Q. Zhou, R.L. Frost, B.J. Wood, L. V. Duong, J.T. Kloprogge, Spectrochim. Acta A, (66) (2007) 1180–1188.